

Efficient thermo-optic phase modulators on an indium phosphide membrane

Yi Wang,¹ Victor Dolores-Calzadilla,^{1,2} Kevin Williams¹, Meint Smit¹ and Yuqing Jiao¹

¹ Institute for Photonic Integration, Eindhoven University of Technology, Eindhoven, 5600MB, the Netherlands

² Photonic Integration Technology Center (PITC), Eindhoven University of Technology, Eindhoven, 5600MB, the Netherlands

In this paper, we present the design and demonstration of thermo-optic phase modulators (TOPM) on the indium phosphide membrane on silicon (IMOS) platform. The TOPM is based on Joule heating of the metal wire on top of a 1 μm thick polyimide planarization layer. Due to the low thermal leakage of the bonding layer, a low P_π of around 7.1 mW has been achieved, comparable to state-of-the-art high-efficiency TOPMs on silicon photonics. The simulated thermal time constant was 14.1 μs . The TOPM has been fabricated and characterized in a Mach-Zehnder interferometer (MZI) configuration.

Introduction

Thermo-optic phase modulators (TOPMs) have been widely proposed in photonic integrated circuits (PICs), whose applications include tunable light source tunable lasers [1], optical switching [2], and sensing [3], [4]. The simple working principle enables TOPMs' easiness of fabrication, low cost, low optical loss, and high reproducibility. Although TOPMs have been extensively studied on the silicon photonics platform, and efficient P_π of several mW [5]–[7] can be readily achieved, it has been challenging to realize such designs on InP-based platforms due to the much larger waveguide dimensions and high thermal leakage through the claddings. However, by substituting the III-V cladding with low-index benzocyclobutene (BCB) material, the InP membrane on silicon (IMOS) platform [8], [9] offers a unique opportunity for realizing efficient TOPMs with tightly confined waveguides and good thermal isolation. The realization of efficient TOPMs on the IMOS platform provides a valuable extension to the existing library of active and passive components. In this paper, the design, simulation, fabrication and characterization of such a TOPM will be discussed.

Design and simulation

As seen in Fig. 1, The TOPM on IMOS is based on Joule heating of a metal wire (often Au) on top of the planarization layer (polyimide, PI). The vertical spacing between the metal wire and the InP waveguide has been set to 1 μm to balance thermal efficiency and optical loss. For the benefit of high fabrication tolerance, the width of the metal wire has been set to 2 μm . The thickness of such metal wire depends on the fabrication, but 300 nm is a typical value. The waveguide dimension has been set to 400 nm \times 300 nm, standard of the IMOS platform [8].

The electro-thermal simulation has been done by the commercial software, COMSOL Multiphysics. In simulation, the length of the metal wire was set to 50 μm , but it can

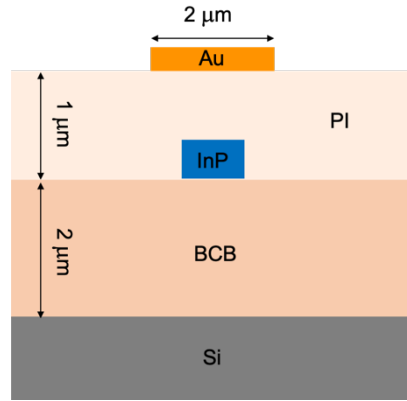


Figure 1. Design of the TOPM on IMOS (cross-sectional view)

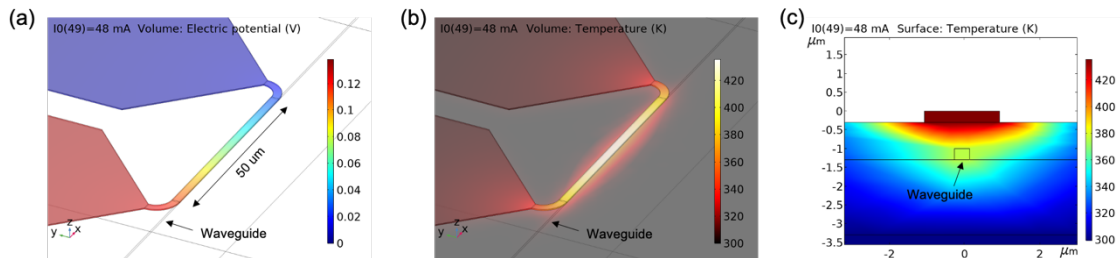


Figure 2. Electro-thermal simulation of the TOPM on IMOS at 48 mA injection current. (a): Electric potential distribution. (b): Temperature distribution. (c): Cross-sectional temperature distribution.

vary depends on application needs. For simplicity, the composition of the metal wire has been set to pure Au. Although in reality the metal wire will consist of Ti/Au, the Ti adhesion layer is too thin to have a significant impact on the wire resistance. The metal pads have been included in the simulation, because they act as heat sinks and significantly influence the simulation results. The bottom of the silicon wafer and the top of the metal pads have been set to room temperature (300 K), and all other boundaries have been set to natural air convection ($h = 5 \text{ W m}^{-2} \text{ K}^{-1}$).

The electric potential and temperature distribution have been calculated at 48 mA injection current, as seen in Fig. 2(a) and (b), respectively. Since here Au heater has been used, its low resistivity facilitates a low driving voltage of $< 0.15 \text{ V}$. As can be seen in Fig. 2(c), a temperature of $\sim 428 \text{ K}$ has been observed in the metal wire. In the core of the waveguide, this value was $\sim 370 \text{ K}$.

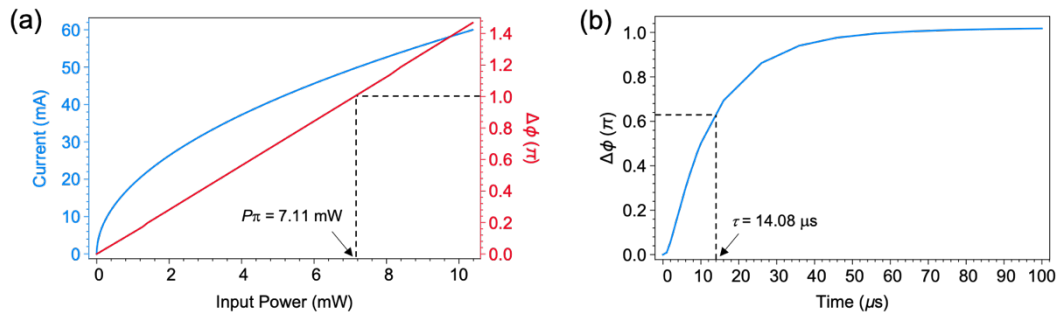


Figure 3. Performance figures of the TOPM (a): Phase shift for 1550 nm wavelength at varying injection current. (b): Transient response of the TOPM when applied power jumps from 0 to P_π (7.11 mW).

To calculate the phase shift based on the temperature distribution, an integration along the waveguide has been performed, using the following equation:

$$\Delta\phi = \int \Delta T(x) \frac{2\pi k_{\text{InP}}}{\lambda} dx,$$

where ΔT is the temperature rise compared to room temperature, λ is the wavelength, k_{InP} is the thermo-optic coefficient and it's equal to $2 \times 10^{-4} \text{ K}^{-1}$ [10] at 300 K for InP. For simplicity, the temperature dependence of k_{InP} [10] has not been taken into consideration. As seen in Fig. 3(a), the phase shift follows a linear relation with the injected power, with the $P_\pi = 7.11 \text{ mW}$ for 1550 nm wavelength. Though absent of design tricks like multi-pass or undercut, this low P_π value is already comparable to state-of-the-art TOPMs on the silicon photonics platform [5], [7]. This natural high efficiency is due to the low thermal leakage through the polymer cladding layers ($\kappa_{\text{BCB}} = 0.29 \text{ W m}^{-1} \text{ K}^{-1}$ and $\kappa_{\text{PI}} = 0.15 \text{ W m}^{-1} \text{ K}^{-1}$, while $\kappa_{\text{SiO}_2} = 1.3 \text{ W m}^{-1} \text{ K}^{-1}$).

Transient results have also been obtained in the simulation, as seen in Fig. 3(b). The rising time can be quantified by the thermal time constant τ , which is the time needed for the phase shift to change 63.2% ($1-1/e$). For our TOPM, τ is equal to $14.08 \mu\text{s}$. The combination of P_π and τ yields a figure of merit (FOM) of $100.1 \text{ mW} \cdot \mu\text{s}$, which is comparable to state-of-the-art high-efficiency TOPMs on silicon photonics [6].

Characterization

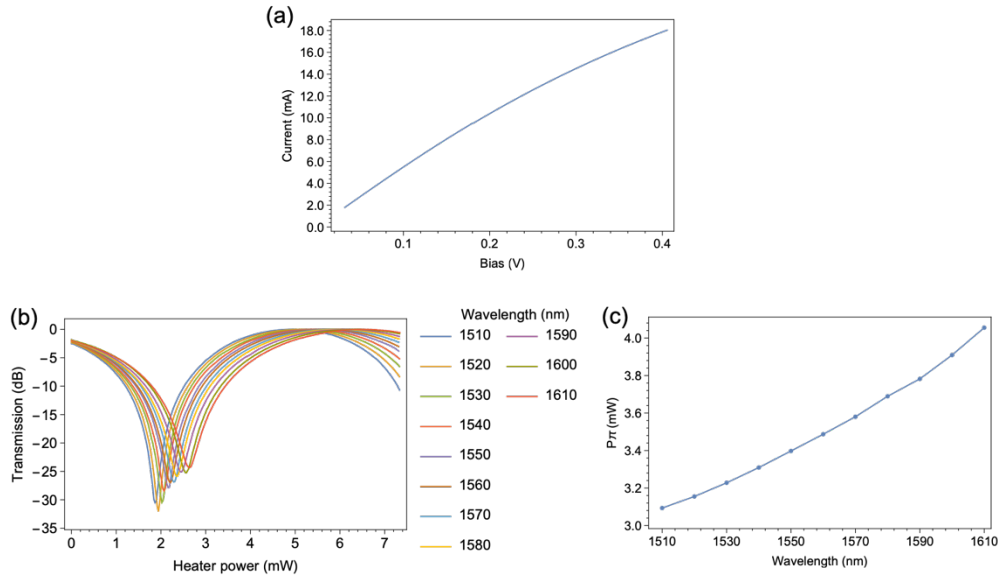


Figure 4. Measurement results of the TOPM with a length of $100 \mu\text{m}$. (a): IV curve of the TOPM. (b): Logarithmic plot of the transmission with varying heater power. (c): Extracted P_π values for different wavelengths.

The chip has been fabricated following the normal IMOS process [11], and on-chip Mach-Zehnder interferometers (MZI) have been used to characterize the performance of the TOPMs. As seen in Fig. 4(a), the IV curve showed ohmic-like behavior with a resistance of around 22Ω . The higher resistance was due to the fact that only 100 nm of Au was used, a value designed to accommodate for other components on the wafer. The transmission of the MZI with varying heater power can be seen in Fig. 4(b), showing a minimum extinction ratio (ER) of around 25 dB . To obtain the power for π phase shift, the transmission data has been fitted with cosine functions in linear scale. The

wavelength-dependent P_π results can be seen in Fig. 4(c). For 1550 nm the value was 3.42 mW, which was significantly smaller than the simulated one (7.11 mW). This was due to problems in planarization during fabrication: the PI layer was etched too much and there was almost no PI on top of the waveguides. Although the fabrication error led to even higher efficiency, it brought the metal too close to the waveguide, and the optical loss measured was more than 700dB/cm.

Conclusion

In this paper, we have presented a TOPM design on the InP membrane platform. Unlike conventional InP platforms which have thick III-V cladding layers and thus inefficient heat delivery/extraction, the InP membrane platform showed promising heat tuning efficiency. In simulation, we have obtained a P_π of 7.11 mW, while in experiment it was 3.42 mW. The significant difference was due to fabrication errors which can be avoided in the future.

References

- [1] R. Wang *et al.*, “Widely Tunable III–V/Silicon Lasers for Spectroscopy in the Short-Wave Infrared,” *IEEE J. Sel. Top. Quantum Electron.*, vol. 25, no. 6, pp. 1–12, Nov. 2019, doi: 10.1109/JSTQE.2019.2924109.
- [2] R. Konoike, K. Suzuki, S. Namiki, H. Kawashima, and K. Ikeda, “Ultra-compact silicon photonics switch with high-density thermo-optic heaters,” *Opt. Express*, vol. 27, no. 7, p. 10332, Apr. 2019, doi: 10.1364/OE.27.010332.
- [3] Jie Sun *et al.*, “Large-Scale Silicon Photonic Circuits for Optical Phased Arrays,” *IEEE J. Sel. Top. Quantum Electron.*, vol. 20, no. 4, pp. 264–278, Jul. 2014, doi: 10.1109/JSTQE.2013.2293316.
- [4] S. A. Miller *et al.*, “Large-scale optical phased array using a low-power multi-pass silicon photonic platform,” *Optica*, vol. 7, no. 1, pp. 3–6, Jan. 2020, doi: 10.1364/OPTICA.7.000003.
- [5] M. R. Watts, J. Sun, C. DeRose, D. C. Trotter, R. W. Young, and G. N. Nielson, “Adiabatic thermo-optic Mach–Zehnder switch,” *Opt. Lett.*, vol. 38, no. 5, p. 733, Mar. 2013, doi: 10.1364/OL.38.000733.
- [6] S. Chung, M. Nakai, and H. Hashemi, “Low-power thermo-optic silicon modulator for large-scale photonic integrated systems,” *Opt. Express*, vol. 27, no. 9, p. 13430, Apr. 2019, doi: 10.1364/OE.27.013430.
- [7] H. Qiu *et al.*, “Energy-efficient thermo-optic silicon phase shifter with well-balanced overall performance,” *Opt. Lett.*, vol. 45, no. 17, p. 4806, Sep. 2020, doi: 10.1364/OL.400230.
- [8] Y. Jiao *et al.*, “Indium Phosphide Membrane Nanophotonic Integrated Circuits on Silicon,” *Phys. Status Solidi A*, vol. 217, no. 3, p. 1900606, Feb. 2020, doi: 10.1002/pssa.201900606.
- [9] J. J. G. M. van der Tol, Y. Jiao, J. P. Van Engelen, V. Pogoretskiy, A. A. Kashi, and K. Williams, “InP Membrane on Silicon (IMOS) Photonics,” *IEEE J. Quantum Electron.*, vol. 56, no. 1, pp. 1–7, Feb. 2020, doi: 10.1109/JQE.2019.2953296.
- [10] F. G. Della Corte, G. Cocorullo, M. Iodice, and I. Rendina, “Temperature dependence of the thermo-optic coefficient of InP, GaAs, and SiC from room temperature to 600 K at the wavelength of 1.5 μm ,” *Appl. Phys. Lett.*, vol. 77, no. 11, pp. 1614–1616, Sep. 2000, doi: 10.1063/1.1308529.
- [11] J. J. G. M. van der Tol *et al.*, “Indium Phosphide Integrated Photonics in Membranes,” *IEEE J. Sel. Top. Quantum Electron.*, vol. 24, no. 1, pp. 1–9, Jan. 2018, doi: 10.1109/JSTQE.2017.2772786.